14th International Symposium on Turbulence and Shear Flow Phenomena (TSFP14)
Heidelberg, Germany, July 28–31, 2026

DNS OF THE PLANE COUETTE FLOW AT HIGH FRICTION RICHARDSON NUMBERS

Victor Avsarkisov
Meteorology, MIN Faculty
Universität Hamburg
20146 Hamburg, Germany
victor.avsarkisov@uni-hamburg.de

Sergio Gandìa-Barberà
Instituto Universitario de Matemàtica Pura y Aplicada
Universitat Politècnica de València,
46022 València, Spain
serganba@etsii.upv.es

Sergio Hoyas
Instituto Universitario de Matemàtica Pura y Aplicada
Universitat Politècnica de València,
46022 València, Spain
serhocal@upvnet.upv.es

ABSTRACT

Stratified turbulence simulated in the plane Couette flow configuration is investigated in the present study. We performed direct numerical simulations of the turbulent flow at a fixed friction Reynolds number and a Prandtl number of air, with a wide range of stratification rates, aiming to study the effects of the stable vertical stratification in this canonical flow configuration. We investigate the flow statistics, nondimensional parameter space, and analyze various turbulent and thermal budgets to conclude that the core region of the flow is governed by the strong mean vertical shear, while the strong stratification effects are mostly confined to the near-wall region.

INTRODUCTION

The physics of stratified sheared flow can be described using a set of non-dimensional parameters, including the molecular Prandtl number, the buoyancy Reynolds number, and the horizontal and vertical Froude numbers (Davidson, 2013; Riley & Lindborg, 2013):

$$Pr = \nu/\kappa, \tag{1}$$

$$R_B = \varepsilon/(\nu N^2), \tag{2}$$

$$Fr_v = u_h/(l_v N), \tag{3}$$

$$Fr_v = u_h/(l_v N), \tag{4}$$

here ν and k are the kinematic viscosity and thermal diffusivity, respectively; ε is the dissipation rate of turbulent kinetic energy; $N = \sqrt{(-g/\rho_0)(\partial\overline{\rho}/\partial z)}$ is the Brunt-Väisälä (buoyancy) frequency; u_h, l_h and l_v are the characteristic horizontal velocity and the corresponding horizontal and vertical length scales of the largest turbulent structure.

In this study, we present DNS of plane Couette flow with a fixed Reynolds number of $Re_\tau = 1000$ and stable thermal stratification. We adjusted the computational box selection to align with the results of our previous DNS at low stratification rates (Gandía-Barberá *et al.*, 2021). These results revealed how the turbulent structure of channel flow changes at these rates. This study further investigates the evolution of the flow in the presence of stronger, stable vertical stratification. To accomplish this, we analyze turbulence statistics, and nondimensional characteristics.

NUMERICAL SIMULATIONS

The streamwise, wall-normal, and spanwise coordinates are represented by x_1, x_2, and x_3, respectively, while the corresponding velocity components are denoted as U_1, U_2, and U_3. Density is indicated by ρ_t. Statistically averaged quantities are represented by an overbar, whereas fluctuating quantities are denoted by lowercase letters. Thus, we have $U_i = \overline{U}_i + u_i$. There is one exception to this notation: since the capital letter ρ can be confused with P, we use a subscript t for density, resulting in $\rho_t = \overline{\rho} + \rho$. The superscript (+) signifies that the quantities have been scaled by the friction velocity and the friction temperature:

$$u_\tau \equiv \sqrt{\nu|\partial\overline{U}_1/\partial x_2|_{\mathrm{wall}}}, \tag{5}$$

$$\Theta_\tau \equiv (\kappa/u_\tau)|\partial\overline{\Theta}/\partial x_2|_{\mathrm{wall}}. \tag{6}$$

The wall velocity, U_w scale all other quantities.

The governing equations of the system are the Navier-Stokes equations under the Boussinesq approximation:

$$\partial_j U_j = 0, \tag{7}$$

$$\partial_t U_i + U_j \partial_j U_i = -\partial_i P + \frac{1}{Re_\tau}\partial_{jj} U_i - Ri_\tau \rho_t \delta_{i2}, \tag{8}$$

$$\partial_t \rho_t + U_j \partial_j \rho_t = \frac{1}{Re_\tau Pr}\partial_{jj}\rho_t. \tag{9}$$

In these equations, Ri_τ represents the Richardson friction number, defined as $Ri_\tau = \Delta\rho g h/\rho_0 u_\tau^2$. Here $\Delta\rho$ is the difference in density between the two walls, with the flow being denser at the bottom wall. Dirichlet boundary conditions are applied to model ρ_t. Additionally, g denotes acceleration due to gravity, and ρ_0 is a reference density. The study utilizes the Prandtl number of air, which is $Pr = 0.71$. The previous equations are transformed to derive an equation for the wall-normal vorticity ω_{x_2} and for the Laplacian of the wall-normal velocity $\phi = \nabla^2 u_2$. For spatial discretization, the method involves dealiased Fourier expansions in the x_1 and x_3 directions, along with seven-point compact finite differences in the x_2 direction, with fourth-order consistency and extended spectral-like resolution (Lele, 1992). The temporal discretization employs a third-order semi-implicit Runge-Kutta scheme (Spalart *et al.*, 1991). The computational code utilized in this research has previously been employed in various studies with different boundary conditions (Hoyas & Jiménez, 2006, 2008; Avsarkisov *et al.*, 2014*a*,*b*; Kraheberger *et al.*, 2018; Lluesma-Rodríguez *et al.*, 2018).

Table 1 summarizes the four new DNSs of turbulent plane Couette flow conducted for this study. The friction Reynolds number remained approximately the same across all simulations, $Re_\tau \equiv u_\tau h/\nu \approx 1000$, while the friction Richardson number, Ri_τ, ranged from 0 to 1000. As the friction Reynolds number, the domain was kept the same, with dimensions $L_{x_1} = 8\pi h, L_{x_2} = 2h, L_{x_3} = 3\pi h$, to contain a pair of rolls (see Alcántara-Ávila *et al.*, 2019). The mesh size was $N_{x_1} = 1536, N_{x_2} = 251, N_{x_3} = 1152$ points, providing a resolution of 8.2 and 4.1 wall units in x_1 and x_3 directions, respectively. The wall-normal grid spacing is adjusted to keep the resolution at $\Delta x_2 = 1.5\eta$, i.e., approximately constant in terms of the local isotropic Kolmogorov scale η. In wall units, Δx_2^+ varies from 0.83 at the wall, up to $\Delta x_2^+ \simeq 2.3$ at the centreline. This grid size is similar to the one typically used in channel flows, for both P- and C- Flows (Hoyas & Jiménez, 2006; Avsarkisov *et al.*, 2014*a*; Lluesma-Rodríguez *et al.*, 2018; Lee & Moser, 2018). In every simulation case, the flow had to evolve from an initial field, which has been taken from a previous case with lower Ri_τ. The code was run until a transition phase was passed and the flow had adjusted to the new set of parameters. The transition is characterized through, among other variables, the value of the shear stress in the moving wall. Once this parameter reaches a plateau, statistics are collected as in García-Villalba & Álamo (2011) and Deusebio *et al.* (2015). In order to further validate the database, the total density flux, which must be equal to one, has been calculated as the sum of the turbulent and molecular density fluxes. The following equation comes from integration of eq. 9,

$$1 = \overline{u_2\rho}^+ - \frac{d\overline{\rho_t}^+}{dx_2^+}, \tag{10}$$

and it is shown in Figure 1.

The total density flux test (Gandía-Barberá *et al.*, 2021), presented in Figure 1, suggests a lack of statistics for the Ri_{500} and Ri_{1000} cases. However, almost 30 wash-outs for the Ri_{500} case and 13 for the Ri_{1000} case (see Table 1) are more than enough for the DNS of canonical channel flow. One possible explanation for this statistical behavior is the intermittent (patchy) nature of the turbulence at these stratification rates, despite the relatively large friction Obukhov scales ($L_{\mathrm{ob}}^+ \equiv u_\tau^4/(\kappa g \alpha_\nu q_w \nu) = L_{\mathrm{ob}} u_\tau/\nu$) shown in Table 1. According to Flores & Riley (2010) and Deusebio *et al.* (2015), the degree of turbulence patchiness may be defined by the value of L_{ob}^+, which must exceed the approximate critical value of $L_{\mathrm{ob}}^+ = 200$. Especially, for the Ri_{1000} case, where $L_{\mathrm{ob}}^+ = 257$, we closely approach this threshold.

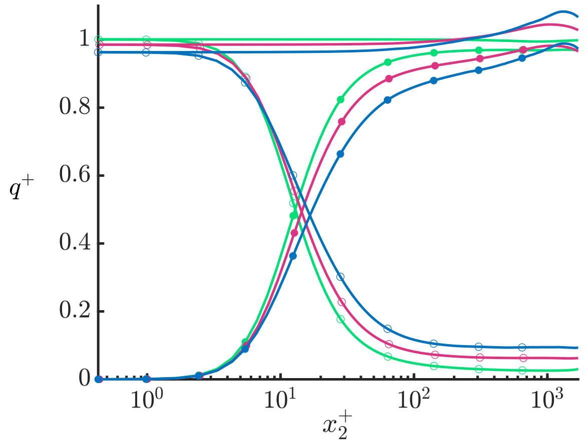

Figure 1. The heat fluxes obtained from the energy balance equation 10. Molecular flux (○), $d\overline{\rho_t}^+/dx_2^+$; turbulent flux (●), $\overline{u_2\rho}^+$; and the total density fluxes in inner scales. Colors are as in Table 1.

RESULTS

Figure 2(*a*, *b*) shows vertical profiles of the mean streamwise velocity and the mean temperature in outer scales (U_w, Θ_w, h). It is already well-known from the literature (Deusebio *et al.*, 2015; García-Villalba & Álamo, 2011; García-Villalba *et al.*, 2011) that with an increase in the stratification, these mean characteristics of the flow approach a linear profile similar to the laminar solution in the core region. This effect is attributed to a reduced turbulent momentum flux generation in the near-wall region under stratification. The damping of the near-wall vortex generation mechanism is another well-known feature of the stably stratified flows. Recently, it has been shown that even weak stratification affects the near-wall vortex generation. It prevents the formation of large-scale vortex rolls in the core region of the turbulent plane Couette flow (Gandía-Barberá *et al.*, 2021). Despite the apparent linear behavior of the mean velocity and temperature profiles, it is misleading to attribute the constant-shear region to the laminar flow. This flow remains dependent on the velocity and temperature stresses at the walls, as it was pointed out in Deusebio *et al.* (2015).

Figure 2(*c*) provides the velocity profiles in an inner scale $(u_\tau, ^+)$. As it follows from the plot, the viscous sublayer (the layer closest to the wall highlighted with the circles' line) is not affected by the buoyancy force up to $x_2^+ = 10$. On the other hand, the near-wall logarithmic layer is obtained only in the plane Couette flow case without stratification and in a one-and-a-half decade range $40 \leqslant x_2^+ \leqslant 1000$. A large log layer, which is half-decade larger than the one simulated in the Poiseuille channel flow at $Re_\tau = 10.000$ $(400 \leqslant x_2^+ \leqslant 2500)$ (Hoyas *et al.*, 2022), is caused by the large-scale streamwise rolls, characteristic of the plane Couette flow without stratification (Tsukahara *et al.*, 2006; Kitoh & Umeki, 2008; Avsarkisov *et al.*, 2014*a*). Velocity profiles for cases with stratification suggest the non-existence of the classic near-wall logarithmic layer in the presence of the wall-normal buoyancy force. Instead, we obtain an extended buffer region in the range $x_2^+ = 10 - 100$. The constant shear-dominated region initiates at approximately $x_2^+ = 100$ and spans across the whole core region of the flow.

Vertical profiles of turbulent root mean square (r.m.s.) velocities are shown in Figure 2(*d*). The near-wall peak of $u_{1,\mathrm{rms}}^+$ does not change its position from the wall $x_2^+ = 14$ and coincides at all stratification rates. However, the strength of

Table 1. Overview of performed simulations. Two different Reynolds and Richardson numbers are provided depending on the moving wall U_w and friction u_τ velocities. The next three columns denote the friction velocity u_τ and the computational period of the collected statistics in eddy turn-overs (u_τ/h) and wash-outs (U_b/L_{x_1}). The final two rows represent the Obukhov scale ($L_{\rm ob} \equiv u_\tau^3/(\kappa g \alpha_v q_w)$) in wall-units and outer scales. Line colors are consistently applied in all plots throughout the paper.

Case	Line	Re_w	Re_τ	Ri_w	Ri_τ	u_τ	Tu_τ/h	TU_b/L_{x_1}	$L^+_{\rm ob}$	$L_{\rm ob}$
Ri_0	grey	25500	1047.40	0.0000	0.00	0.0411	23.74	20.81	∞	∞
Ri_{100}	green	43500	991.72	0.0617	96.20	0.0228	11.28	17.81	1045	1.053
Ri_{500}	magenta	74000	1010.80	0.1086	471.65	0.0137	11.15	29.39	390	0.385
Ri_{1000}	blue	95000	987.55	0.1272	953.17	0.0104	3.80	13.15	257	0.265

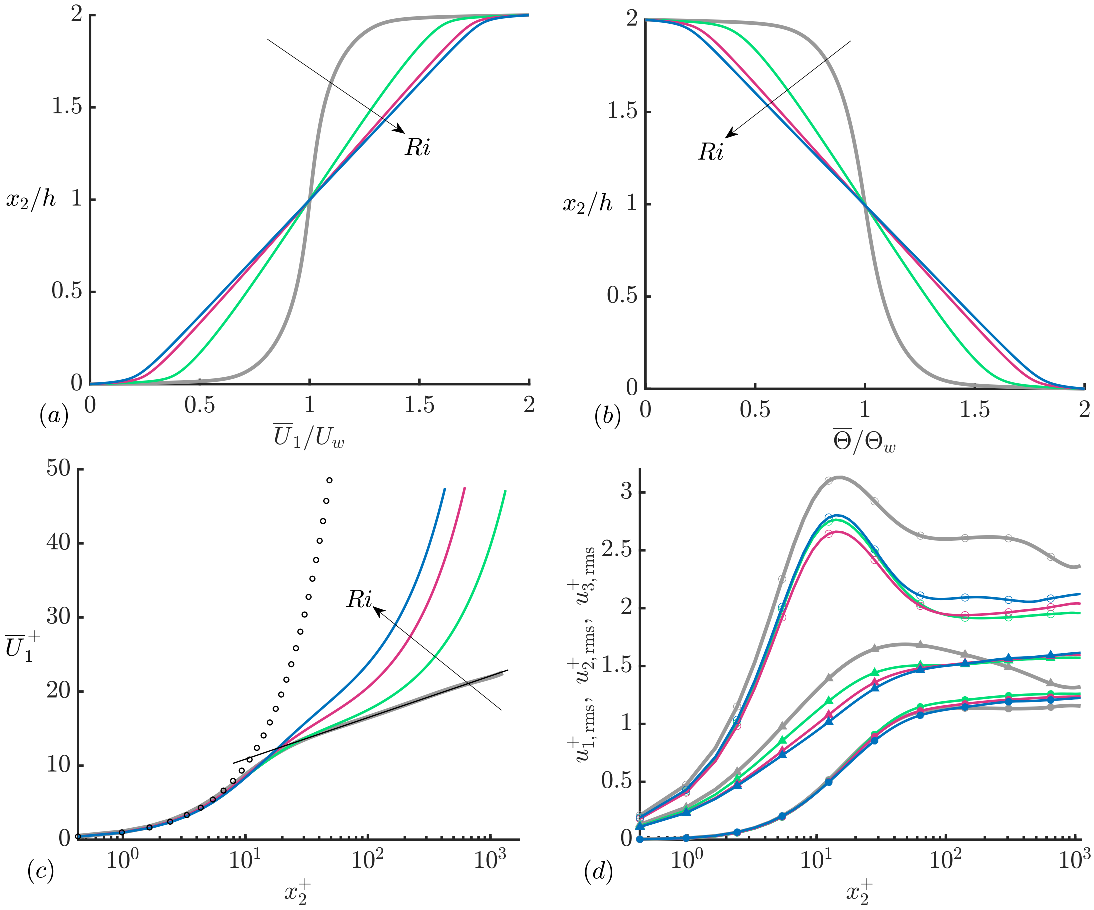

Figure 2. Vertical profiles of (*a*) mean velocity and (*b*) mean temperature scaled in outer (U_w, Θ_w, h) scales. The stratification rate is increasing in the arrow direction. (*c*) Mean velocity profiles scaled in inner scales ($u_\tau, ^+$). The viscous sublayer linear scaling law ($\circ$), $\overline{U}_1^+ = x_2^+$; the thin black solid line corresponds to the near-wall logarithmic scaling law $\overline{U}_1^+ = 1/0.41\log(x_2^+) + 5.25$; (*d*) Vertical profiles of r.m.s. (root mean square) velocities in inner scale: ($\circ$), $u_{1,\rm rms}/u_\tau$; ($\bullet$), $u_{2,\rm rms}/u_\tau$; ($\blacktriangle$), $u_{3,\rm rms}/u_\tau$. Colors are as in Table 1.

this peak decreases by $10-13\%$ compared to the unstratified case in all simulations with stratification. These conclusions align well with other DNS results from Deusebio *et al.* (2015); García-Villalba & Álamo (2011). The present study shows that the strength of the peak is approximately constant for all *Ri* and *Re* cases, that is $u^+_{1,\rm rms} = 2.6-2.7$, including cases analyzed in Deusebio *et al.* (2015); García-Villalba & Álamo (2011) (see Figures 4(*a*) and 7(*a*) therein, respectively). The near wall peak of the $u^+_{3,\rm rms}$ component disappears with the increase of stratification rate. The decrease of the $u^+_{3,\rm rms}$ in the center of the channel observed in the unstratified case develops into the plateau with stratification. The collapse of all three $u^+_{3,\rm rms}$ profiles in the region $x_2^+ = 100-1000$ suggests the constant shear domination. While the collapse of $u^+_{2,\rm rms}$ profiles at the wall $x_2^+ \leqslant 10$ is evidence of the presence of viscous sublayer in all (unstratified and stratified) DNS cases.

The buoyancy Reynolds number, defined using only the vertical component of the turbulent dissipation $R_B = \varepsilon_v/(\nu N^2)$, where $\varepsilon_v = |\varepsilon_{22}|$, is plotted in Figure 3(*a*). There is a steep increase in R_B in the near-wall region and a reach of saturation in the core region with a constant velocity shear rate. One can observe the effect of increasing stratification by the decrease in the R_B value in the plateau region, which fills over 90% of the channel. All three simulation cases with stratification exhibit the buoyancy Reynolds numbers larger than the threshold value of $R_B = 20$ (Smyth & Moum, 2000), indicating the existence of a stationary turbulent regime in the flow. The vertical profiles of the R_B are very similar to the ones shown in García-Villalba *et al.* (2011), with only one exception. Namely, there are no near-wall peaks at low stratification rates, as in García-Villalba *et al.* (2011, Fig. 3*a*).

The horizontal Froude numbers, defined as $Fr_h = \varepsilon_v/(Nu_h^2)$, are plotted in Figure 3(*b*). After exhibiting a peak in the near-wall region, Fr_h shows relaxation towards the channel center and builds a plateau for the case with the strongest stratification. As expected, the values of Fr_h decrease with stratification, indicating an increase in the horizontal-to-vertical integral scale anisotropy resulting from stratification. However, none of the simulated cases reach a strongly stratified turbulence regime $Fr_h < 0.02$, as formulated in Lindborg (2006).

The turbulent Reynolds number defined as $Re_T = R_B/Fr_h^2$ is plotted in Figure 3(*c*). Here again, we observe a reduction in the turbulence rate of the flow with stratification. Although Re_T is commonly used to define the turbulence state in flows, we do not recommend using it for stratified, sheared, turbulent channel flows. R_B, Fr_h, and the Obukhov scale in wall-units L_{ob}^+ (see Table 1) are much more extensively verified state metrics for flows with stable stratification.

The vertical Froude number $Fr_v = L_b/l_v$ is plotted in Figure 3(*d*). An increase of Fr_v with stratification suggests that the vertical integral scale l_v is approaching the buoyancy scale, $L_b = u_h/N$, with stratification. In the strongly stratified turbulence regime, it is expected that the vertical Froude number will reach unity. In the present DNS study, however, we could only reach $Fr_v = 0.5$ in the core region.

Figure 3(*e*) shows the vertical profile of the gradient Richardson number $Ri_g = N^2/S^2$, where $S \equiv d\overline{U}_1/dx_2$ is the mean vertical shear of the streamwise velocity, while $\overline{U}_1$ is the mean streamwise velocity. It indicates that Ri_g increases with stratification. Similar to Fr_h, the gradient Richardson number defines the strength of stratification in the flow and exhibits behavior that resembles saturation plateau. Considering the rapid decrease of R_B with stratification, it is highly plausible that Fr_h will only reach values of 0.14 or 0.15 in the Couette channel flow configuration. This result corroborates the observation by Zhou *et al.* (2017) that a strongly stratified state (as interpreted by Lindborg (2006), $R_B > 10-20$, $Fr_h < 0.02$), cannot be achieved in a plane Couette flow.

However, the present DNS simulations reveal a peculiar implication regarding the relationship between the gradient Richardson number and the horizontal Froude number. It is well-known that scaling of the square of the mean shear rate relates the Ri_g, R_B, and Fr_h parameters to each other. As previously demonstrated in the literature, when S^2 is dominated by integral scales (shear-dominated scenario) and $S \sim u_h/l_h$, we obtain

$$Ri_g \sim Fr_h^{-2}. \tag{11}$$

Alternatively, when the flow is dominated by the dissipation scales and $S \sim u_\eta/l_\eta$, here $u_\eta = (\nu\varepsilon)^{1/4}$ and $l_\eta = (\nu^3/\varepsilon)^{1/4}$, we would have (Davidson, 2013):

$$Ri_g \sim R_B. \tag{12}$$

However, as Figure 3(*a*, *b*, *e*) shows, the behavior of R_B, Fr_h, and Ri_g does not follow either of these scenarios. The primary reason for this is the scaling failure of the mean shear rate and thermal rate at strong stratification in the core region of the flow. Using the characteristic horizontal velocity u_h and the vertical Ozmidov scale defined as $L_{ozv} = \sqrt{\varepsilon_v/N^3}$, for $\partial\overline{U}_1/\partial x_2$ and with the rms-temperature $\theta_{\rm rms}$ and L_{ozv} for $\partial\overline{\Theta}/\partial x_2$ yields increasingly better scaling at strong stratification. A corresponding relationship between Ri_g and Fr_h obtained at these scaling behaviors is

$$Ri_g = \frac{N^2}{(d\overline{U}_1/dx_2)^2} \sim \frac{N^2}{u_h^2/L_{ozv}^2} = \frac{N^2}{u_h^2}\left(\sqrt{\frac{\varepsilon_v}{N^3}}\right)^2 = \frac{\varepsilon_v}{u_h^2 N} \sim Fr_h. \tag{13}$$

A key implication of scaling (13) is that the gradient Richardson number may exhibit a similar threshold of $Ri_g \sim Fr_h \approx 0.15$ in turbulent plane Couette flows under strong stratification ($Ri_\tau \approx 1000$ and higher). However, to validate this idea, additional direct numerical simulations with stronger stratification rates are needed.

Finally, Figure 3(*f*) illustrates another significant nondimensional parameter, the flux Richardson number Ri_f. This is defined as:

$$Ri_f = \frac{(g/\rho_0)\overline{\rho u_2}}{\overline{u_1 u_2} d\overline{U}_1/dx_2}, \tag{14}$$

where $-(g/\rho_0)\overline{\rho u_2}$ is the buoyancy flux, and $-\overline{u_1 u_2} d\overline{U}_1/dx_2$ is the shear production.

It shows the ratio of buoyant destruction to shear production within the turbulent kinetic energy equation. Similarly to the gradient Richardson number, Ri_f increases with stratification and reaches a plateau in the core region. Furthermore, the values at the plateau are proportional to the values of Ri_g for different stratification strengths. This result is consistent with analyses by Zhou *et al.* (2017).

CONCLUSION

In the present study, we perform direct numerical simulations of the plane Couette flow with stable vertical stratification at a fixed high friction Reynolds number and various stratification rates (see Table 1). The present study aimed to simulate the strongly stratified regime in a simple channel flow configuration; however, our results suggest that this is probably unachievable. A similar conclusion was previously made by Zhou *et al.* (2017) and García-Villalba *et al.* (2011). In our understanding, this is not possible due to the novel scaling relation between the gradient Richardson number and the horizontal Froude number that emerges under strong stratification (see eq. (13)). The primary cause of this scaling is the emergence of the vertical Ozmidov scale as a characteristic scale for the mean velocity and temperature gradient in the core region. Being much smaller than the characteristic integral vertical scale ($l_v = u_v^3/\varepsilon_v$) and the buoyancy scale ($L_b = \overline{U}_1/N$), this indicates that small-scale turbulence is limited to these vertical distances.

REFERENCES

Alcántara-Ávila, F., Gandía-Barberá, S. & Hoyas, S. 2019 Evidences of persisting thermal structures in Couette flows. *International Journal of Heat and Fluid Flow* **76**, 287–295.

Avsarkisov, V., Hoyas, S., Oberlack, M. & García-Galache, J.-P. 2014*a* Turbulent plane Couette flow at moderately high reynolds number. *J. Fluid Mech.* **751**, R1.

Avsarkisov, V., Oberlack, M. & Hoyas, S. 2014*b* New scaling laws for turbulent Poiseuille flow with wall transpiration. *J. Fluid Mech.* **746**, 99–122.

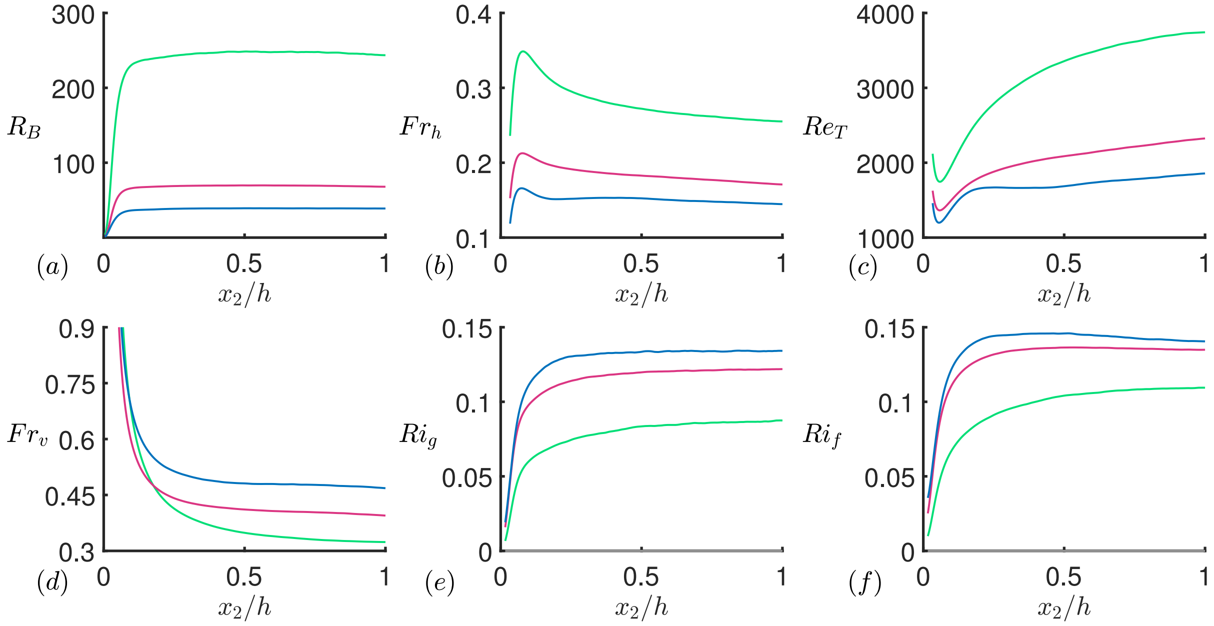

Figure 3. Vertical profiles of (a) the buoyancy Reynolds number R_B; (b) the horizontal Froude number Fr_h; (c) the turbulent Reynolds number R_T; (d) the vertical Froude number Fr_v; (e) the gradient Richardson number Ri_g; and (f) the flux Richardson number Ri_f. The colors are as in Table 1.

Davidson, P. A. 2013 *Turbulence in Rotating, Stratified and Electrically Conducting Fluids*. Cambridge University Press.

Deusebio, E., Caulfield, C. P. & Taylor, J. R. 2015 The intermittency boundary in stratified plane Couette flow. *J. Fluid Mech.* **781**, 298–329.

Flores, O. & Riley, J. J. 2010 Analysis of turbulence collapse in stably stratified surface layers using direct numerical simulation. *Bound. Layer Met.* **129** (2), 241–259.

Gandía-Barberá, S., Alcántara-Ávila, F., Hoyas, S. & Avsarkisov, V. 2021 Stratification effect on extreme-scale rolls in plane Couette flows. *Phys. Rev. Fluids* **6**, 034605–1–18.

García-Villalba, M & Álamo, Juan C. Del 2011 Turbulence modification by stable stratification in channel flow. *Phys. Fluids* **23**, 045104–1–22.

García-Villalba, M, Azarga, E. & Uhlmann, M. 2011 A numerical study of turbulent stably-stratified plane Couette flow. *High Performance Computing in Science and Engineering* **10**, 251–261.

Hoyas, S. & Jiménez, J. 2006 Scaling of the velocity fluctuations in turbulent channels up to $re_\tau = 2003$. *Phys. Fluids* **18** (1), 011702.

Hoyas, S. & Jiménez, J. 2008 Reynolds number effects on the Reynolds-stress budgets in turbulent channels. *Phys. Fluids* **20** (10), 101511.

Hoyas, S., Oberlack, M., Alcántara-Ávila, F., Kraheberger, S. V. & Laux, J. 2022 Wall turbulence at high friction Reynolds numbers. *Phys. Rev. Fluids* **7**, 014602–1–10.

Kitoh, O. & Umeki, M. 2008 Experimental study on large-scale streak structure in the core region of turbulent plane Couette flow. *Phys. Fluids* **20** (2), 025107.

Kraheberger, S., Hoyas, S. & Oberlack, M. 2018 Dns of a turbulent couette flow at constant wall transpiration up to $Re_\tau = 1000$. *J. Fluid Mech.* **835**, 421–443.

Lee, M. & Moser, R. 2018 Extreme-scale motions in turbulent plane Couette flows. *J. Fluid mech.* **842**, 128–145.

Lele, S. K. 1992 Compact finite difference schemes with spectral-like resolution. *J. Comp. Phys.* **103** (1), 16–42.

Lindborg, E. 2006 The energy cascade in a strongly stratified fluid. *J. Fluid Mech.* **550**, 207–242.

Lluesma-Rodríguez, F., Hoyas, S. & Peréz-Quiles, M.J. 2018 Influence of the computational domain on DNS of turbulent heat transfer up to $Re_\tau = 2000$ for $Pr = 0.71$. *International Journal of Heat and Mass Transfer* **122**, 983–992.

Riley, J. J. & Lindborg, E. 2013 Recent progress in stratified turbulence. In *Ten Chapters in Turbulence* (ed. P. A. Davidson, Y. Kaneda & K. R. Sreenivasan), pp. 269–317. Cambridge University Press.

Smyth, W. D. & Moum, J. N. 2000 Anisotropy of turbulence in stably stratified mixing layers. *Phys. Fluids* **12**, 1343–1362.

Spalart, P. R., Moser, R. D. & Rogers, M. M. 1991 Spectral methods for the Navier-Stokes equations with one infinite and two periodic directions. *J. Comp. Phys.* **96** (2), 297–324.

Tsukahara, T., Kawamura, H. & Shingai, K. 2006 DNS of turbulent Couette flow with emphasis on the large-scale structure in the core region. *J. Turbulence* **7** (N19), 1–16.

Zhou, Q., Taylor, J. R. & Caulfield, C. P. 2017 Self-similar mixing in stratified plane Couette flow for varying Prandtl number. *J. Fluid Mech.* **820**, 86–120.